Supporting Information

Boron-rich Enhanced Ambient CO_2 Capture and Storage of Boron-Carbon-Nitride Hybrid Nanotubes

Fatemeh Ershadi[1], Farzaneh Shayeganfar[1,2*], Ali Ramazani[3]

[1]Department of Physics and Energy Engineering, Amirkabir University of Technology, Tehran
[2]Department Aerospace Engineering, University of Michigan, Ann Arbor, MI 10485, USA
[3]Department of Mechanical Engineering, Massachusetts Institute of Technology, Cambridge, MA 02139, USA

Contents

* fshayeganfar@aut.ac.ir
fshayega@umich.edu

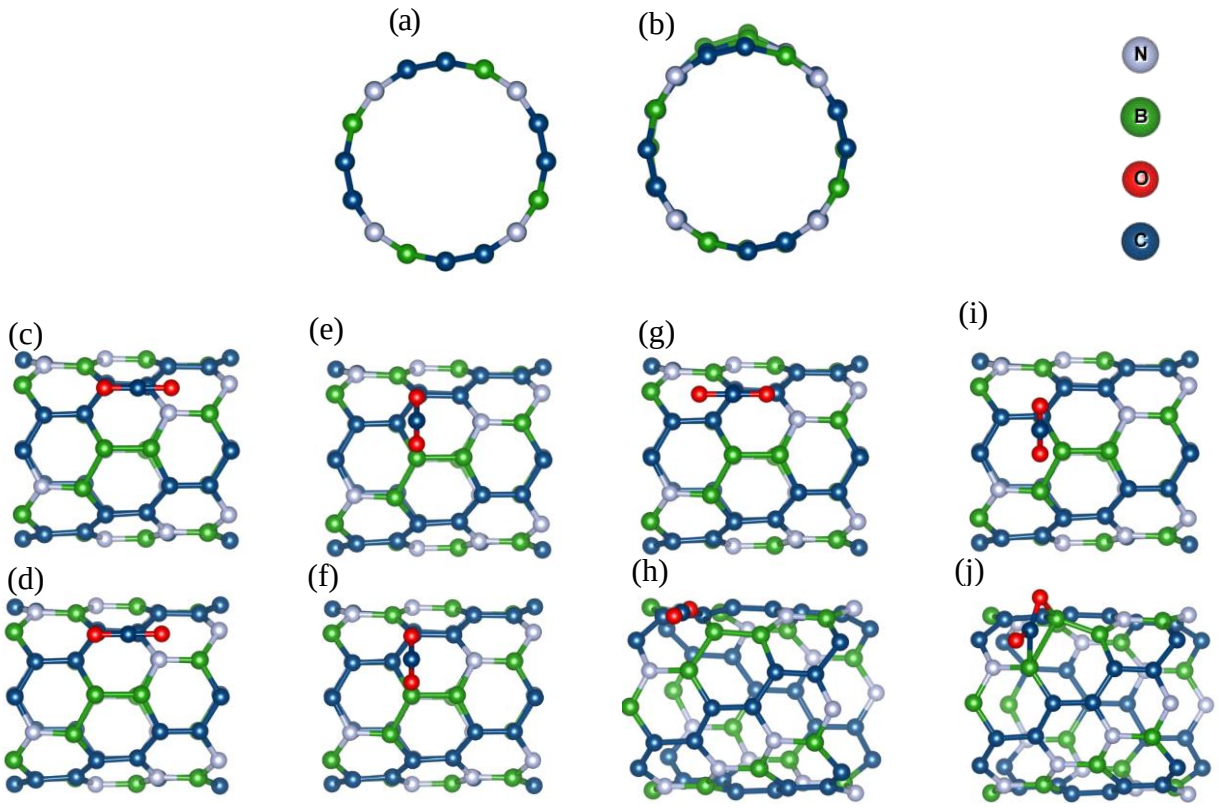

Figure S1. (a) The geometric configurations are three-row BC_2NNT (8,0) without CO_2 before relaxation and (b) after relaxation. (c) Adsorption of CO_2 on the B_N site, where the O atom is located above the B_N site and parallel to the nanotube axis before and (d) after relaxation, (e) the O atom is located above the B_N site and oblique to the nanotube axis before and (f) after relaxation, (g) C of CO_2 is top of B_N parallel to the nanotube axis before and (h) after relaxation, (i) C of CO_2 is top of B oblique to the nanotube axis before and (j) after relaxation.

Table S1. Comparison of adsorption energy in nanotubes with three-row and single-row unit cells in BC_2NNT

	Single-row BC_2NNT unit cell E_{ads}	**Three rows BC_2NNT unit cell E_{ads}**
O up B_N-Parallel	-0.63 eV	-0.35 eV
O up B_N-Oblique	-0.42 eV	-0.21 eV
C up B_N-Parallel	-0.63 eV	-0.34 eV
C up B_N-Oblique	-2.52 eV	-1.12 eV

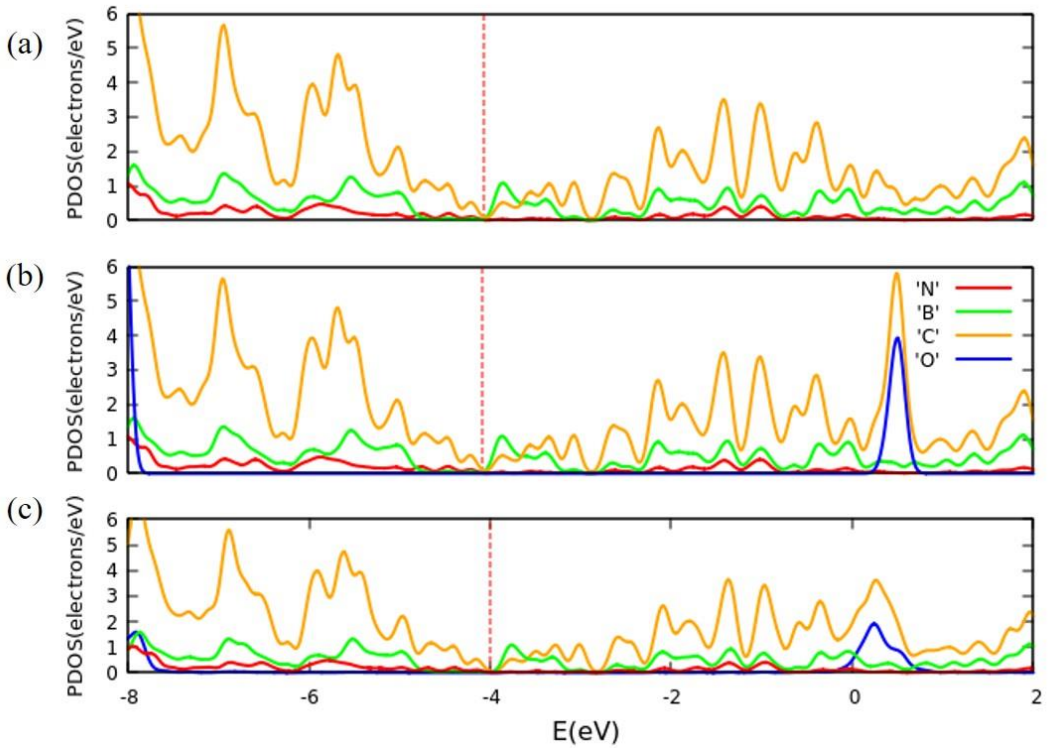

Figure S2. PDOS of BC_4NNT (8,0) for (a) isolated nanotube, (b) where CO_2 is at 4.6 Å far from the nanotube. (c), for the physisorption process where the C atom is located above the B_N-parallel site. The red dashed lines show the Fermi level.

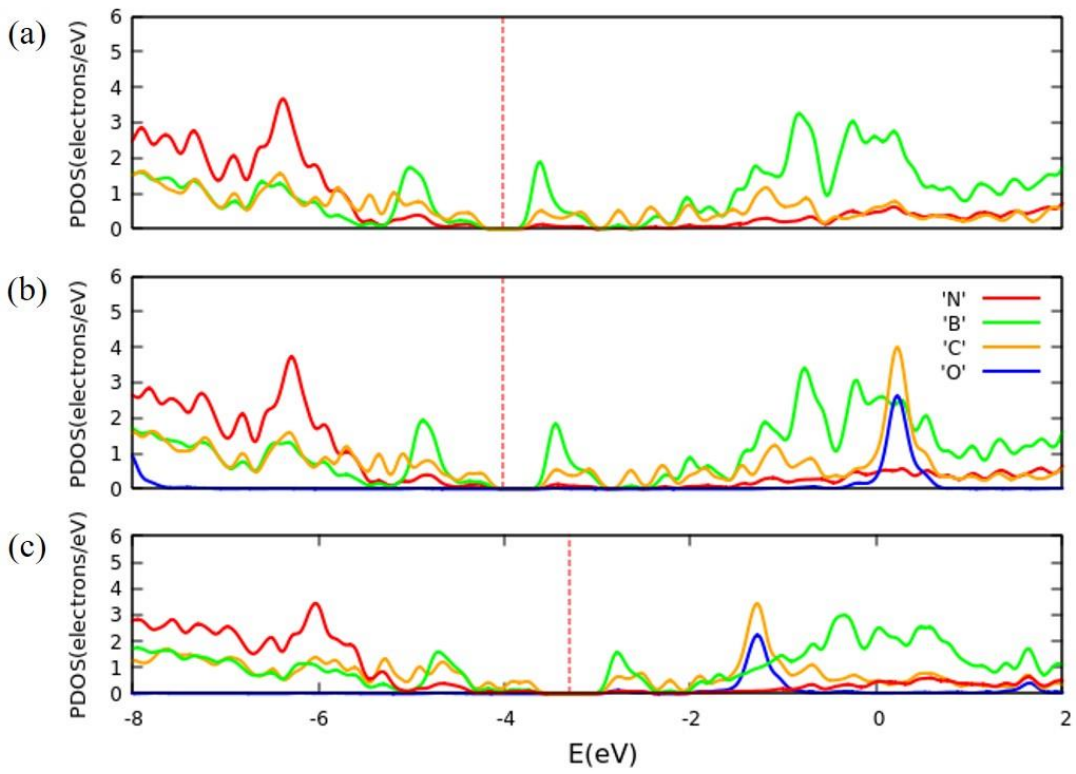

Figure S3. PDOS of p-BNCNT (8,0) nanotube for (a) isolated nanotube, (b) where CO_2 is at 5 Å far from the nanotube. (c), for the physisorption process where the C atom is located above the B_N-oblique site. The red dashed lines show the Fermi level.

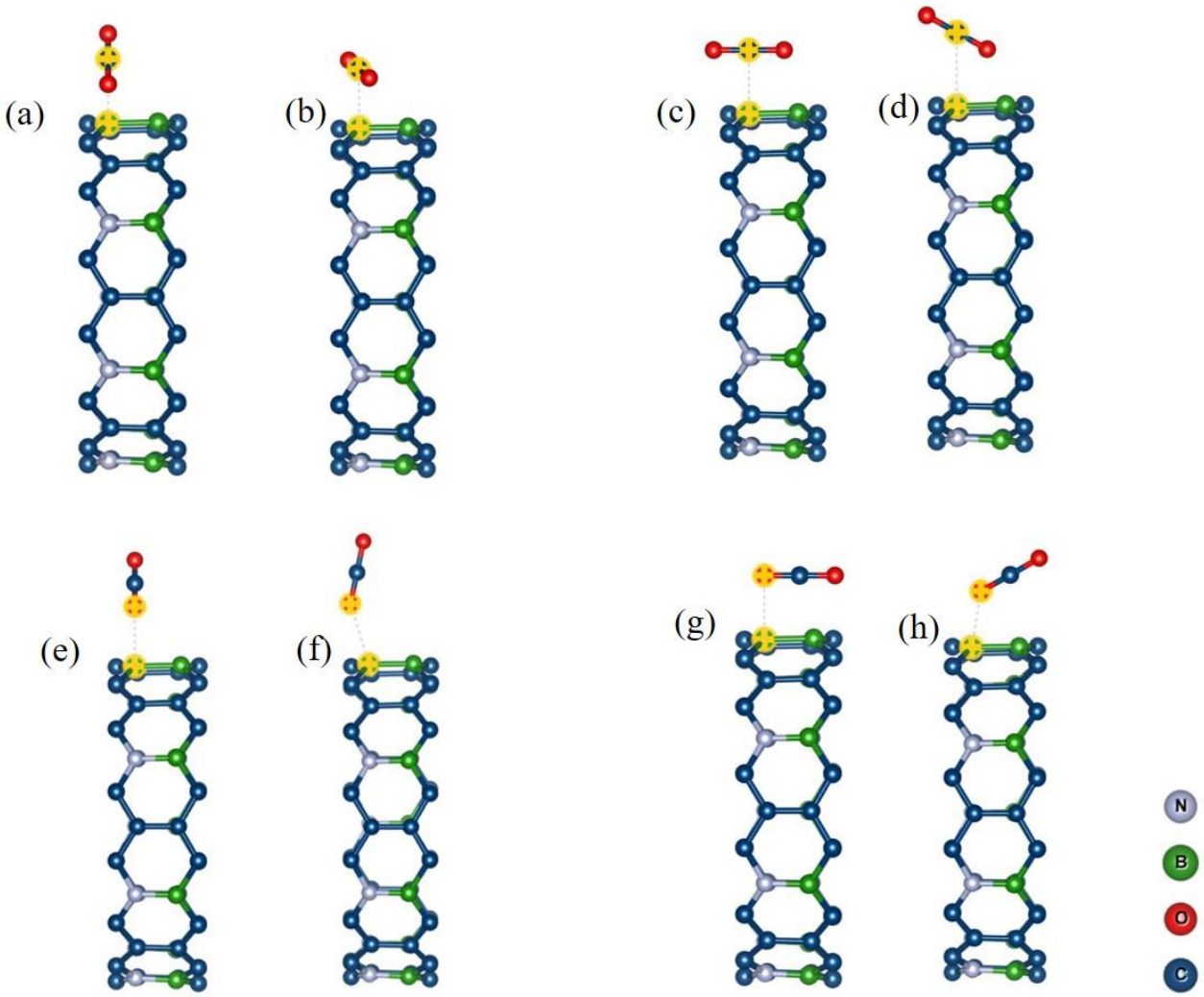

Figure S4. The geometric configurations of single-row BC_4NNT (14,0). (a) The adsorption of CO_2 where the C atom is located above B_N site and oblique to the nanotube axis before and (b) after relaxation, the C atom is located above B_N site and parallel to the nanotube axis (c) before and (d) after relaxation, O atom is located above B_N site and oblique to the nanotube axis (e) before and (f) after relaxation, the O atom is located above B_N site and parallel to the nanotube axis (g) before and (h) after relaxation.

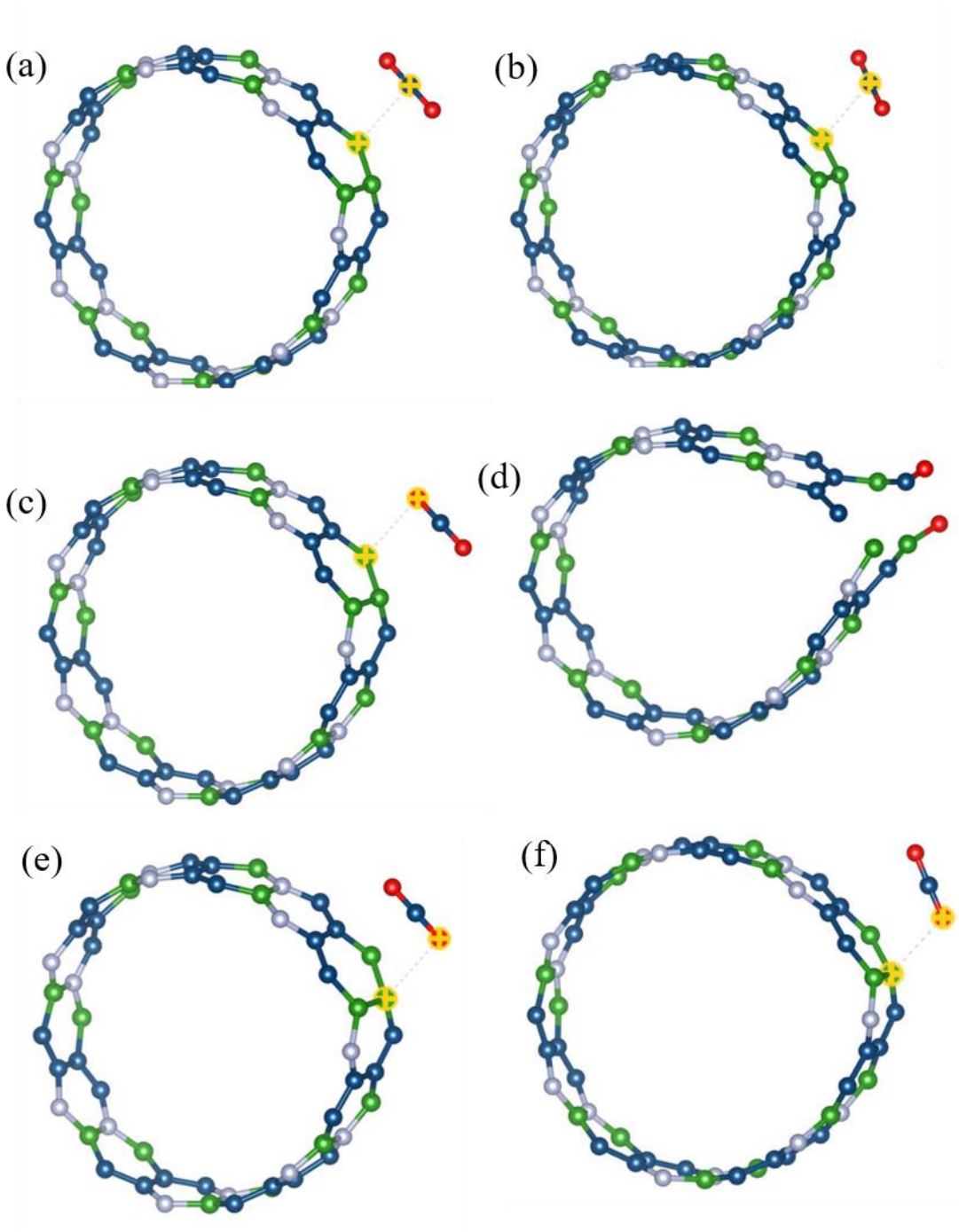

Figure S5. The geometric configurations of single-row BC_2NNT (14,0). (a) The adsorption of CO_2 where the C atom is located above B_N site and oblique to the nanotube axis before and (b) after relaxation, the O atom is located above B_N site and oblique to the nanotube axis (c) before and (d) after relaxation, O atom is located above B site and oblique to the nanotube axis (e) before and (f) after relaxation.

Table S2. Comparing the recovery time of CO_2 adsorption in different sites of BC_2NNT.

Recovery time	Adsorption energy	Structure
0.0488 s	-0.635 eV	C up B_N-parallel (BC_2NNT)-8-0
3.44×10^{30} s	-2.527 eV	C up B-oblique (BC_2NNT)-8-0
0.04770 s	-0.634 eV	O up B_N-parallel (BC_2NNT)-8-0
1.26×10^{-4} s	-0.422 eV	O up B_N-oblique (BC_2NNT)-8-0

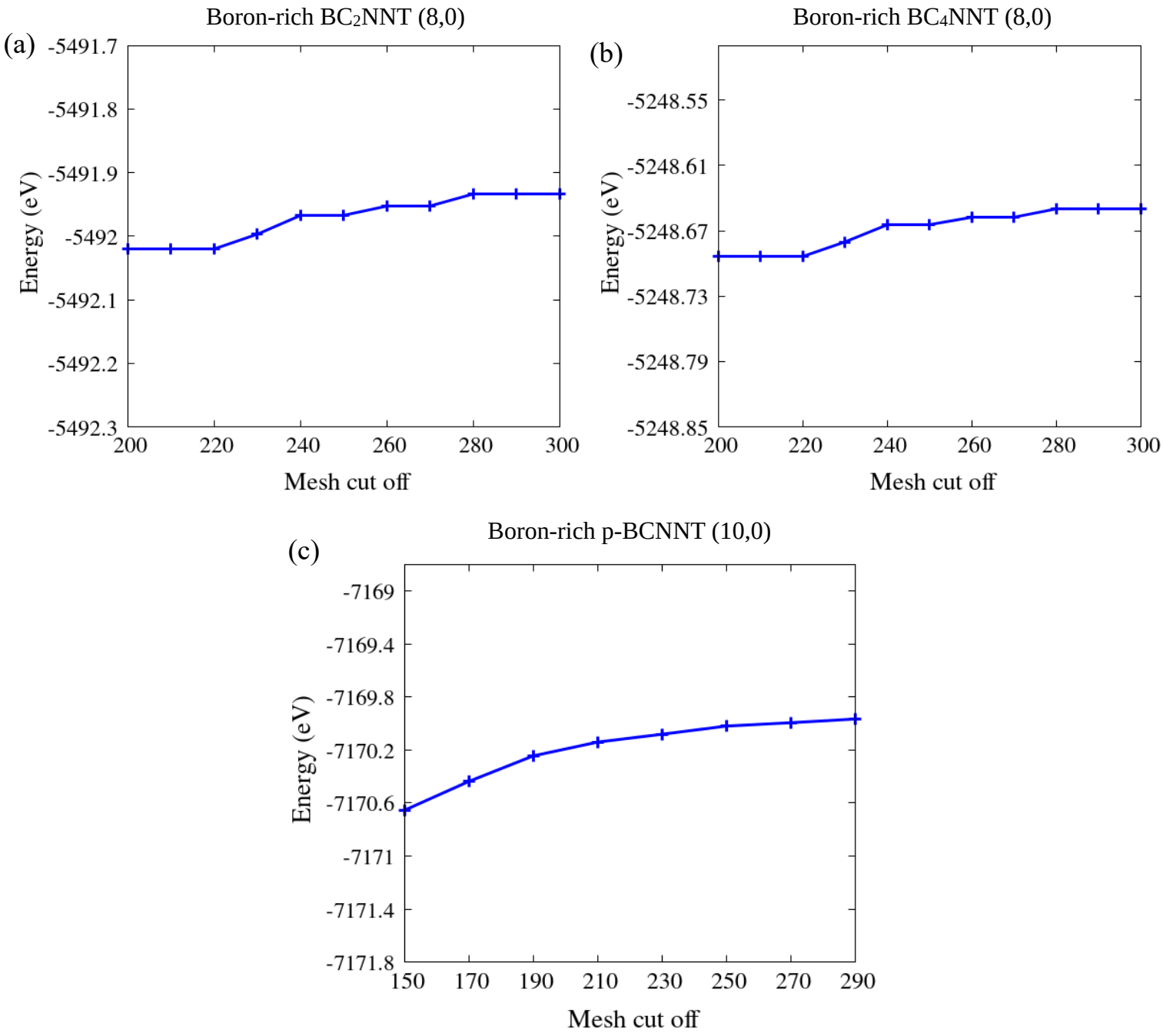

Figure S6. Mesh cut-off optimization plot of (a) BC_2NNT (8,0), (b) BC_4NNT (8,0), and (c) BCNNT (10,0)